

## Flavor decomposition for the proton unpolarized, helicity and transversity parton distribution functions

---

Constantia Alexandrou,<sup>a,b</sup> Martha Constantinou,<sup>c</sup> Kyriakos Hadjiyiannakou,<sup>a,b</sup>  
Karl Jansen<sup>d</sup> and Floriano Manigrasso<sup>a,e,f,\*</sup>

<sup>a</sup>Department of Physics, University of Cyprus, P.O. Box 20537, 1678 Nicosia, Cyprus

<sup>b</sup>Computation-based Science and Technology Research Center, The Cyprus Institute, 20 Kavafi Str., Nicosia 2121, Cyprus

<sup>c</sup>Temple University, 1925 N. 12th Street, Philadelphia, PA 19122-1801, USA

<sup>d</sup>NIC, Deutsches Elektronen-Synchrotron, 15738 Zeuthen, Germany

<sup>e</sup>Institut für Physik, Humboldt-Universität zu Berlin, Newtonstr. 15, 12489 Berlin, Germany

<sup>f</sup>Dipartimento di Fisica, Università di Roma "Tor Vergata", Via della Ricerca Scientifica 1, 00133 Rome, Italy

E-mail: [manigrasso.floriano@ucy.ac.cy](mailto:manigrasso.floriano@ucy.ac.cy)

We present an *ab initio* calculation of the individual up, down, and strange quark unpolarized, helicity, and transversity parton distribution functions for the proton. The calculation is performed within the Wilson twisted mass clover-improved fermion formulation in lattice QCD. We use a  $N_f = 2 + 1 + 1$  gauge ensemble simulated with pion mass  $m_\pi \approx 260$  MeV,  $m_\pi L \approx 3.8$  and lattice spacing  $a \approx 0.0938$  fm. Momentum smearing is employed in order to improve the signal-to-noise ratio, allowing for the computation of the matrix elements up to nucleon boost momentum of  $P_3 = 1.24$  GeV. The lattice matrix elements are non-perturbatively renormalized and the final results are presented in the  $\overline{MS}$  scheme at a scale of 2 GeV (unpolarized and helicity) and  $\sqrt{2}$  GeV (transversity).

*The 38th International Symposium on Lattice Field Theory, LATTICE2021 26th-30th July, 2021  
Zoom/Gather@Massachusetts Institute of Technology*

---

\*Speaker

## 1. Introduction

Parton distribution functions are key quantities for understanding the structure of hadrons in terms of their constituents. They depend only on the momentum fraction carried by the partons and can be obtained from a number of scattering processes [1, 2]. However, not all distributions are well-constrained from global analysis. The helicity and in particular the transversity proton PDFs can be obtained with much lower precision from experimental data compared to the unpolarized distributions. In addition, the strange-quark distributions are poorly constrained from phenomenology [3–6] and large uncertainties on this quantity affect the determination of the  $W$ -boson mass and the CKM matrix element  $V_{cs}$  [7, 8]. In recent years, the first computations of the disconnected contributions to the nucleon charges and form factors have been achieved [9–14], using gauge ensembles simulated with quark masses fixed to approximately their physical values. Such advancement has been made possible thanks to continuous improvement on computational capabilities, but also on algorithmic development. In particular, the hierarchical probing algorithm [15] significantly improves the quality of the signal. In Ref. [16] we indeed showed that this technique is successful in increasing the signal-to-noise ratio of non-local operator as well, and therefore we employ it in this work to compute the isoscalar disconnected and strange matrix elements.

In this paper, we report our effort in extracting the  $x$ -dependence of the proton unpolarized, helicity and transversity distributions for each quark flavor, employing the quasi-PDF approach [17, 18]. The computation is performed on a  $N_f = 2 + 1 + 1$  clover-improved twisted mass fermions gauge ensemble generated by the Extended Twisted Mass Collaboration (ETMC) [19]. The lattice volume is  $V = 32 \times 64$  and the lattice spacing  $a \approx 0.0938$  fm. The pion mass is  $m_\pi \approx 260$  MeV and  $m_\pi L \approx 3.8$ . For further details see Ref. [19].

## 2. Disconnected contributions

The most challenging aspect of this work is the evaluation of the disconnected quark loops with a Wilson line in the boosted frame. The latter can be written as

$$\begin{aligned} \mathcal{L}^{\text{u+d}}(\tau; z; \Gamma) &= \sum_{\vec{y}} \text{Tr} [(\mathcal{G}_u(y; y+z) + \mathcal{G}_d(y; y+z)) \Gamma W(z)] \\ &= \sum_{\vec{y}} \text{Tr} [\bar{\psi}(y+z) \Gamma W(z) \psi(y)] , \end{aligned} \tag{1}$$

where the trace in the second line is intended for spin, color and flavor indices. In particular, to evaluate the unpolarized and helicity disconnected loops we employed the generalized one-end trick, while the standard one-end trick was used for the transversity matrix elements [21, 22]. Furthermore, to reduce the computational cost coming from the evaluation of the trace in Eq. (1), we employ stochastic techniques and in particular the *hierarchical probing* algorithm [15]. The latter performs a partitioning of the lattice with  $2^{d(k-1)+1}$  Hadamard vectors, where  $d = 4$  is the number of dimensions of the lattice. Contamination to the trace coming from off-diagonal terms is then drastically reduced up to the probing distance  $2^k$  with  $k = 3$ . To further reduce the off-diagonal contamination in spin-color, we apply full dilution in the corresponding subspaces [23]. Moreover, with small quark masses, the contribution to the loops coming from the low modes of the spectrum of the Dirac operator can be sizeable and can therefore contribute substantially to the stochastic

noise [24]. Therefore, we compute the first  $N_{\text{ev}} = 200$  eigen-pairs of the squared Dirac operator  $\mathcal{M}_u \mathcal{M}_u^\dagger$ , that allow to reconstruct exactly the low-modes contribution to the disconnected quark loops. The stochastic techniques described above are, thus, applied to the deflated operator, to evaluate the high-modes contribution to the traces.

The connected and disconnected matrix elements all contain non-local operators with the length of the Wilson line extending up to half the spatial extent of the lattice. We boost the proton at three different momenta, namely  $P_3 = 0.41, 0.83, 1.24$  GeV. In addition, to check for convergence with the boost, we also compute the disconnected unpolarized, helicity and transversity matrix elements for  $P_3 = 1.65$  GeV with the same statistics as the previous smaller boost, i.e.  $\approx 10^6$  measurements. Although providing useful insights regarding the convergence with  $P_3$ , the number of statistics is not sufficient to obtain the same statistical accuracy as for the lower momenta.

### 3. Disconnected matrix elements

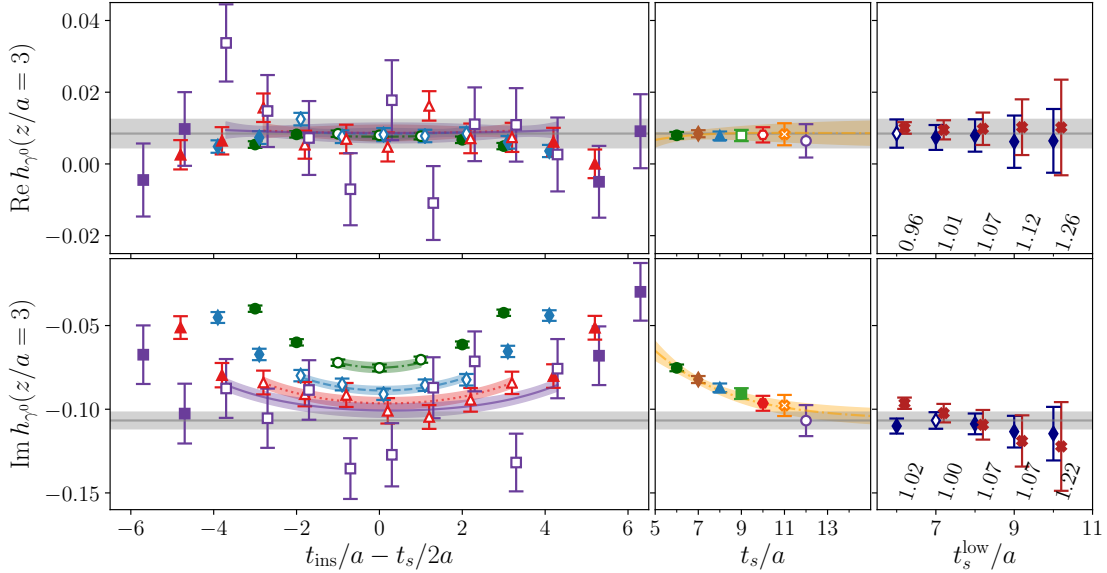


**Figure 1:** Left: Results on  $C_{3pt}(t; t_s)/C_{2pt}(t)$  for the unpolarized PDFs for  $P_3 = 1.24$  GeV, at  $t_s/a = 6$  (green), 8 (blue), 10 (red), 12 (purple) for  $z/a = 3$ . The data for  $t_s/a = 7, 9, 11$  are omitted to improve the readability. The two-state fit results (gray band), and the value of the two-state fit of the three-point function evaluated at the same  $t_s$  as the data-points are also shown. Only the data-points with open symbols are taken into account in the two-state fit procedure. Center: the plateau fit results as a function of  $t_s/a$ . Each source-sink separation is associated with a different color. The orange band is the predicted  $t_s$  dependence of the three-point function. Our final value for the matrix elements is determined as the correlated constant fit of the plateau values shown with open symbols. Right: results of the two-state fit (navy blue) as a function of the lowest source-sink separation  $t_s^{\text{low}}$  included in the fit. The open data-point is the selected two-state fit result, which corresponds to the gray band. For each  $t_s^{\text{low}}$  we report the reduced  $\chi^2$  of the two-state fit. The results obtained with the summation method are reported with the red open crosses as a function of  $t_s^{\text{low}}$ .

To reliably extract the disconnected contributions to the up-, down-, and strange-quark PDFs, we perform an in-depth analysis of the excited states contamination. In particular, we evaluate

the ratio between the three- and two-point functions at seven source-sink separations ranging from  $t_s = 0.563$  fm to  $t_s = 1.126$  fm in steps of  $a = 0.0938$  fm. For the disconnected contribution, the evaluation of different source-sink separations does not require new inversions. To analyze the excited-states contamination to the matrix elements using several  $t_s$  values we employ three analysis methods: plateau fit, two-state fit and summation method. For a concise description of the three techniques we refer to Ref. [25]. In Fig. 1, we show an example of the evaluation of the excited-states contamination affecting the unpolarized disconnected isovector matrix elements at  $P_3 = 1.24$  GeV and  $z/a = 3$ , being  $z$  the Wilson line length. The real part of the matrix elements show no substantial dependence on the source-sink separation, and the plateau fit results obtained at different  $t_s$  give all compatible results. In contrast, the imaginary part shows a large effect due to the excited-states contamination. However, the two-state fit result is compatible with the plateau value obtained at  $t_s/a = 11$ . The summation method provides as well results in agreement with the plateau value. The behavior of the helicity matrix elements with  $t_s$  is very different, indeed the real part shows substantial excited-states contamination while the imaginary part does not depend on  $t_s$  within uncertainties. Regarding the transversity matrix elements, both the real and the imaginary parts show very mild dependence on the source-sink separation. In all cases, we are able to obtain compatible results between the three analysis methods and we extract our final estimate of the matrix elements with the plateau fit analysis at  $t_s/a = 9, 10, 9$  ( $t_s = 11, 10, 9$ ) for the real (imaginary) part of the unpolarized, helicity and transversity, respectively. Indeed, the plateau value extracted from these source-sink separations is compatible with the results from the two-state fit and summation method.

### 3.1 Momentum dependence

The matrix elements and the quasi-PDFs have a dependence on the nucleon boost  $P_3$ . In particular, a crucial aspect of this study is the analysis of the momentum dependence of the matrix elements, which affects the convergence to the light-cone PDFs. We perform a non-perturbative renormalization of the bare disconnected matrix elements obtained with the procedure reported in Sec. 3. In particular, we employ the non-singlet renormalization function, as the difference with the singlet is expected to be small [26]. We apply the regularization independent scheme (RI'), and use the momentum source method [27], offering high statistical accuracy. More detail on the renormalization setup employed in this study can be found in Refs. [28, 29]. In Fig. 2, we show the results for the renormalized strange matrix elements as a function of the nucleon boost. For the unpolarized case, the real part gets suppressed in magnitude as  $P_3$  increases, and at the highest boost becomes compatible with zero. In contrast, the imaginary part increases in magnitude with the nucleon boost, and shows convergence as the boost increases. The first results for the helicity matrix elements appeared in Ref. [16]. Here we show the results with increased statistics, and the addition of  $P_3 = 1.65$  GeV. The imaginary part arises entirely from the complex multiplication of the bare matrix elements with the renormalization function  $Z$ , since the disconnected contribution to the bare helicity matrix elements is purely real. The real part in contrast is significantly non-zero and shows a mild residual dependence on  $P_3$ . Finally, the real part of the matrix elements for the transversity distribution exhibit a strong dependence on the nucleon boost, changing dramatically as we increase  $P_3$  from 0.83 GeV to 1.24 GeV. However, we obtain agreement between the results at the two highest boost values, albeit with large uncertainties. It is still unclear if full convergence is reached, and to

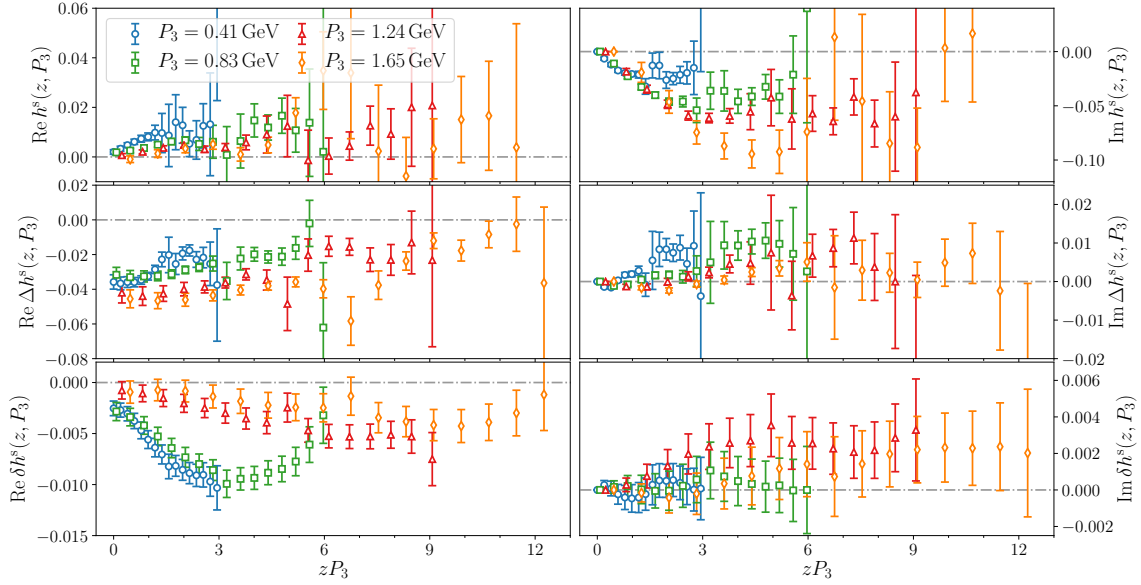


**Figure 2:** Momentum dependence of the renormalized matrix elements for the strange unpolarized (top panel), helicity (middle panel) and transversity (bottom panel) distributions. We show the matrix elements computed at  $P_3 = 0.41$  GeV (blue),  $0.83$  GeV (green),  $1.24$  GeV (red) and  $1.65$  GeV (yellow). Data points are slightly shifted to improve readability.

obtain a clear picture on the momentum dependence of the transversity disconnected matrix elements results at higher boosts with sufficient accuracy would be necessary. This is however beyond the current study and will be tested in a followup work. We, thus, reconstruct the distributions using the results at  $P_3 = 1.24$  GeV. Finally, we find that the isoscalar disconnected matrix elements share the same qualitative behavior as the strange-quark ones shown in Fig. 2.

## 4. Flavor decomposition

### 4.1 Light quark distributions

Combining the results for the disconnected matrix elements, reported in the previous section, with the connected contributions we were able to obtain the light quark PDFs. The computation of the connected isoscalar and isovector contributions is well established. Therefore, we omit the details that can be found in Ref. [25]. In Fig. 3, we show the comparison with phenomenological results of the up and down unpolarized, helicity and transversity distributions. We stress that this comparison can be only quantitative at the current stage since many systematic effects (e.g. larger-than-physical pion mass, cut-off effects) still need to be addressed. The results for the unpolarized PDF are compared with the data by NNPDF3.1 [30], while the helicity distribution is compared with JAM17 [31] and NNPDF<sub>POL1.1</sub> [1]. Finally, the quark transversity distribution obtained in this study is compared against the SIDIS data [32] and SIDIS data constrained by the value of the tensor charge  $g_T$  computed in lattice QCD [32].

The light-quark unpolarized PDFs show good agreement with phenomenology in the region  $0.2 \lesssim x \lesssim 0.5$ . Also, in the region  $x \lesssim -0.2$  our estimate and phenomenology are both compatible

with zero. The lattice results for the small- $x$  region suffer from uncontrolled uncertainties due to cut-off systematic effects. The helicity distribution shows non-negligible contribution from the

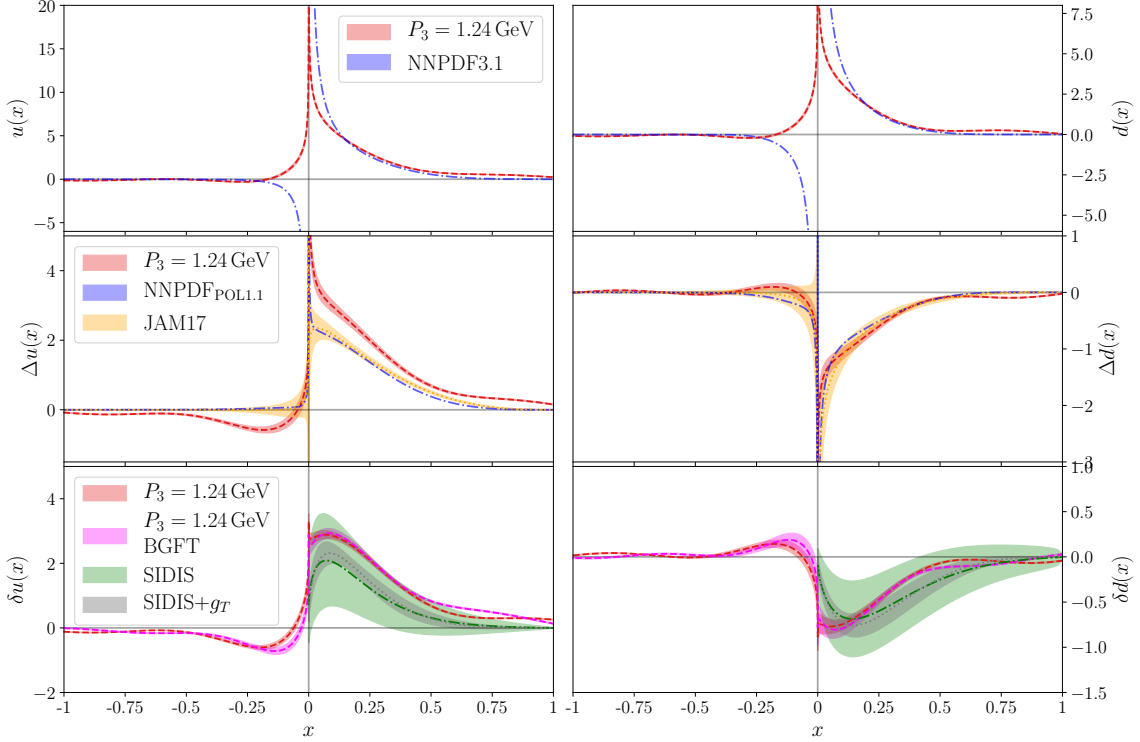


**Figure 3:** Up (left) and down (right) quark unpolarized (upper panels), helicity (middle panels) and transversity (bottom panels) distributions at  $P_3 = 1.24$  GeV (red band). We also show the NNPDF results [1, 30, 33] (blue band) and JAM17 [31] (orange band) phenomenological results. For the transversity PDF we compare against the SIDIS data [32] (green band) and SIDIS data constrained by the value of tensor charge  $g_T$  computed in lattice QCD [32] (gray band). For the transversity distributions we also include the results obtained with the BGFT technique [34] (magenta).

disconnected quark loop. Our results for the up quark helicity show similar features as the NNPDF data, but they are not compatible with the latter within uncertainties. In contrast, the down quark distribution gives compatible results with both NNPDF<sub>POL3.1</sub> and JAM17 data in the entire physical region  $x \in [-1, 1]$ . Finally, the transversity distribution, which is the least known collinear PDF, is compatible with phenomenology. In Fig. 3 we included the light-cone obtained with the Bayes-Gauss Fourier transform [34], an advanced reconstruction technique replacing the discrete Fourier Transform that is able to reduce the artifacts introduced by the discretization of the Wilson line in the Fourier transform. An important observation is that the measurement of this quantity we provide here is more accurate than the experimental one, which carries  $\approx 50 - 100\%$  error [32].

## 4.2 Strange quark distributions

The strange quark distributions are shown in Fig. 4. By increasing the nucleon boost, the unpolarized PDF moves towards the phenomenological results. However, there is still some residual dependence on  $P_3$ , which would require further investigation to be performed in a followup work.

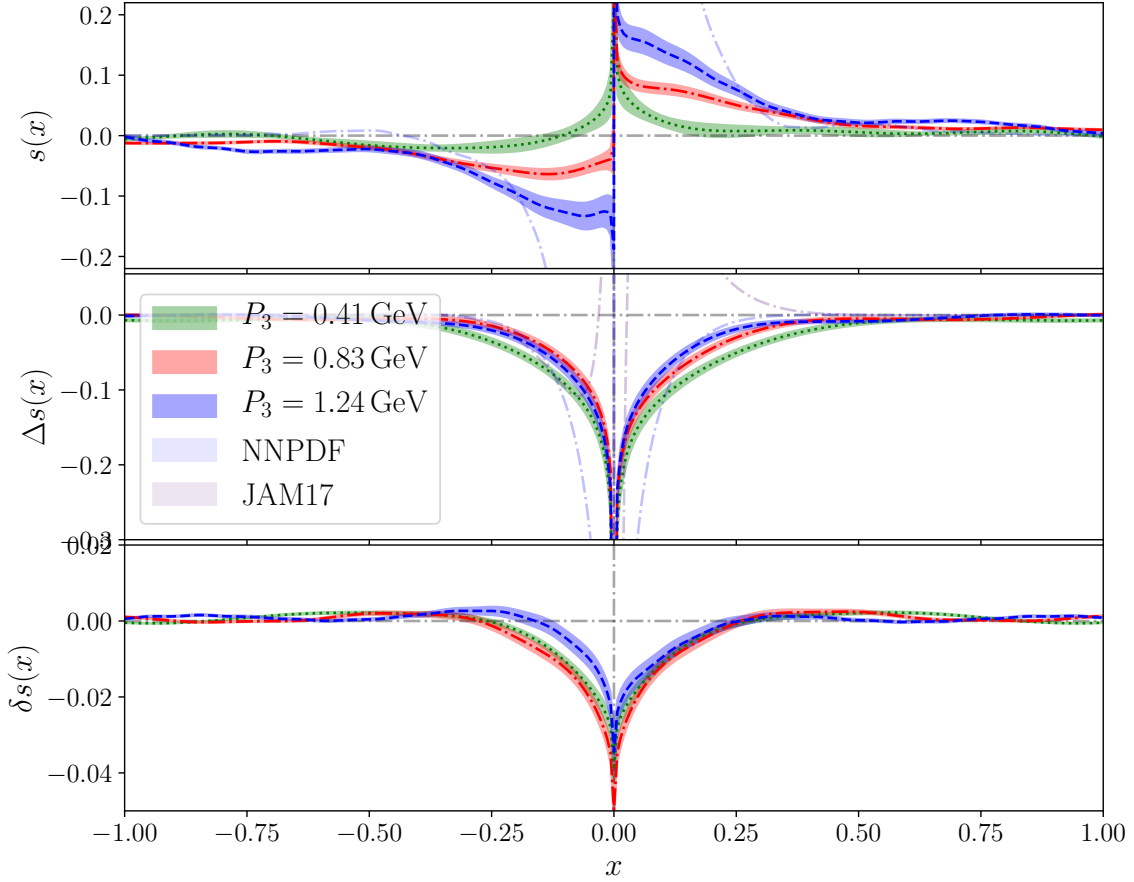


**Figure 4:** Results on the strange unpolarized (top panel), helicity (center panel) and transversity (bottom panel) distributions for three values of  $P_3$ . We compare with the NNPDF<sub>POL1.1</sub> [1, 33] (light blue) and JAM17 [31] (light purple) phenomenological data. Lattice data for  $P_3 = 0.41, 0.83, 1.24$  GeV are shown with green, red and dark blue bands, respectively.

The results for the helicity distribution are approximately symmetric in the quark and antiquark regions, and are compatible with NNPDF<sub>POL1.1</sub> [1] and with JAM17 [31] global fits analysis, both of which have larger uncertainties. Thus, our results constitute valuable input for phenomenological studies. This is particularly evident for the strange transversity distribution, where experimental results are lacking. Our results for the transversity PDF show small uncertainties as well as no residual momentum dependence.

## 5. Conclusions

This work represents a proof-of-principle of the feasibility of the calculation of disconnected quark loops with non-local operators. In particular, we present a study of the  $x$ -dependence of proton collinear quark PDFs from lattice QCD considering both connected and disconnected diagrams. The calculation is carried out on a gauge ensemble of  $N_f = 2 + 1 + 1$  twisted mass fermions with a pion mass of  $m_\pi \approx 260$  MeV. We address excited-states contamination and convergence with the momentum boost in the final PDFs. The proton states are boosted at  $P_3 = 0.41, 0.83, 1.24$  GeV

and several values of the source-sink separation are considered, up to  $t_s = 1.13$  fm. All matrix elements are renormalized multiplicatively using the RI'MOM scheme and evolved to the modified- $\overline{\text{MS}}$  scheme at a scale of 2 GeV (unpolarized and helicity) or  $\sqrt{2}$  GeV (transversity), where different scales are employed to compare with results from phenomenology. The quasi-PDF, obtained with a discrete Fourier transform, is then matched to the light-cone PDFs in the  $\overline{\text{MS}}$  scheme at the same scale. We neglect the mixing with the gluon PDFs for the unpolarized and helicity case, that will be included in future studies.

We find that the light-quark disconnected contributions have the most impact for the helicity PDF, while the transversity disconnected contribution is very small. Nevertheless, we obtain a clear non-zero signal for all kinds of PDFs. Moreover, our results for the unpolarized have a statistical precision which is compatible to the phenomenological data, while the helicity strange-quark PDF is significantly more accurate than the JAM and NNPDF results. Finally, our results for the strange-quark transversity PDF serve, at this stage, as a prediction. In future studies we plan to quantify and eliminate systematic uncertainties, such as pion mass dependence, mixing under matching with the gluon PDFs for the unpolarized and helicity case, finite-volume and discretization effects. Nevertheless, this study clearly demonstrates the potential in the extraction of the  $x$ -dependence of individual quark PDFs from lattice QCD simulations.

## 6. Acknowledgments

We would like to thank all members of ETMC for their constant and pleasant collaboration. We also thank Fernanda Steffens and Jeremy Green for useful discussions. M.C. acknowledge financial support by the U.S. Department of Energy Early Career Award under Grant No. DE-SC0020405. K.H. is supported financially by the Cyprus Research and Innovation Foundation under contract number POST-DOC/0718/0100 and EuroCC project funded by the Deputy Ministry of Research, Innovation and Digital Policy and the Cyprus Research and Innovation Foundation and the European High-Performance Computing Joint Undertaking (JU) under grant agreement No 951732. This project has received funding from the Marie Skłodowska-Curie European Joint Doctorate program STIMULATE of the European Commission under grant agreement No 765048; F.M. is funded under this program. This research includes calculations carried out on HPC resources of the Cyprus Institute (the Cyclone and Cyclamen machines) and of Temple University, supported in part by the National Science Foundation through major research instrumentation grant number 1625061 and by the US Army Research Laboratory under contract number W911NF-16-2-0189. Computations for this work were carried out in part on facilities of the USQCD Collaboration, which are funded by the Office of Science of the U.S. Department of Energy. This research used resources of the Oak Ridge Leadership Computing Facility, which is a DOE Office of Science User Facility supported under Contract DE-AC05-00OR22725. The gauge configurations have been generated by the Extended Twisted Mass Collaboration on the KNL (A2) Partition of Marconi at CINECA, through the Prace project Pra13\_3304 "SIMPHYS".

## References

- [1] E. R. Nocera *et al.* [NNPDF], Nucl. Phys. B **887** (2014), 276-308 doi:10.1016/j.nuclphysb.2014.08.008 [arXiv:1406.5539 [hep-ph]].
- [2] J. J. Ethier and E. R. Nocera, Ann. Rev. Nucl. Part. Sci. **70** (2020), 43-76 doi:10.1146/annurev-nucl-011720-042725 [arXiv:2001.07722 [hep-ph]].

- [3] D. de Florian, R. Sassot, M. Stratmann and W. Vogelsang, *Phys. Rev. D* **80** (2009), 034030 doi:10.1103/PhysRevD.80.034030 [arXiv:0904.3821 [hep-ph]].
- [4] E. Leader, A. V. Sidorov and D. B. Stamenov, *Phys. Rev. D* **82** (2010), 114018 doi:10.1103/PhysRevD.82.114018 [arXiv:1010.0574 [hep-ph]].
- [5] F. Arbabifar, A. N. Khorramian and M. Soleymaninia, *Phys. Rev. D* **89** (2014) no.3, 034006 doi:10.1103/PhysRevD.89.034006 [arXiv:1311.1830 [hep-ph]].
- [6] E. Leader, A. V. Sidorov and D. B. Stamenov, *Phys. Rev. D* **84** (2011), 014002 doi:10.1103/PhysRevD.84.014002 [arXiv:1103.5979 [hep-ph]].
- [7] S. Alekhin, J. Blümlein and S. Moch, *Phys. Lett. B* **777** (2018), 134-140 doi:10.1016/j.physletb.2017.12.024 [arXiv:1708.01067 [hep-ph]].
- [8] M. Aaboud *et al.* [ATLAS], *Eur. Phys. J. C* **78** (2018) no.2, 110 [erratum: *Eur. Phys. J. C* **78** (2018) no.11, 898] doi:10.1140/epjc/s10052-017-5475-4 [arXiv:1701.07240 [hep-ex]].
- [9] C. Alexandrou, S. Bacchio, M. Constantinou, J. Finkenrath, K. Hadjiyiannakou, K. Jansen, G. Koutsou and A. Vaquero Aviles-Casco, *Phys. Rev. D* **100** (2019) no.1, 014509 doi:10.1103/PhysRevD.100.014509 [arXiv:1812.10311 [hep-lat]].
- [10] C. Alexandrou, S. Bacchio, M. Constantinou, J. Finkenrath, K. Hadjiyiannakou, K. Jansen, G. Koutsou and A. Vaquero Aviles-Casco, *Phys. Rev. D* **102** (2020) no.5, 054517 doi:10.1103/PhysRevD.102.054517 [arXiv:1909.00485 [hep-lat]].
- [11] C. Alexandrou, S. Bacchio, M. Constantinou, J. Finkenrath, K. Hadjiyiannakou, K. Jansen, G. Koutsou, H. Panagopoulos and G. Spanouides, *Phys. Rev. D* **101** (2020) no.9, 094513 doi:10.1103/PhysRevD.101.094513 [arXiv:2003.08486 [hep-lat]].
- [12] T. Bhattacharya *et al.* [PNDME], *Phys. Rev. D* **92** (2015) no.9, 094511 doi:10.1103/PhysRevD.92.094511 [arXiv:1506.06411 [hep-lat]].
- [13] J. Liang, M. Sun, Y. B. Yang, T. Draper and K. F. Liu, *Phys. Rev. D* **102** (2020) no.3, 034514 doi:10.1103/PhysRevD.102.034514 [arXiv:1901.07526 [hep-ph]].
- [14] D. Djukanovic, K. Ottnad, J. Wilhelm and H. Wittig, *Phys. Rev. Lett.* **123** (2019) no.21, 212001 doi:10.1103/PhysRevLett.123.212001 [arXiv:1903.12566 [hep-lat]].
- [15] A. Stathopoulos, J. Laeuchli and K. Orginos, [arXiv:1302.4018 [hep-lat]].
- [16] C. Alexandrou, M. Constantinou, K. Hadjiyiannakou, K. Jansen and F. Manigrasso, *Phys. Rev. Lett.* **126** (2021) no.10, 102003 doi:10.1103/PhysRevLett.126.102003 [arXiv:2009.13061 [hep-lat]].
- [17] X. Ji, *Phys. Rev. Lett.* **110** (2013), 262002 doi:10.1103/PhysRevLett.110.262002 [arXiv:1305.1539 [hep-ph]].
- [18] X. Ji, *Sci. China Phys. Mech. Astron.* **57** (2014), 1407-1412 doi:10.1007/s11433-014-5492-3 [arXiv:1404.6680 [hep-ph]].
- [19] C. Alexandrou, S. Bacchio, P. Charalambous, P. Dimopoulos, J. Finkenrath, R. Frezzotti, K. Hadjiyiannakou, K. Jansen, G. Koutsou and B. Kostrzewa, *et al.* *Phys. Rev. D* **98** (2018) no.5, 054518 doi:10.1103/PhysRevD.98.054518 [arXiv:1807.00495 [hep-lat]].
- [20] C. Alexandrou and C. Kallidonis, *Phys. Rev. D* **96**, no.3, 034511 (2017) doi:10.1103/PhysRevD.96.034511 [arXiv:1704.02647 [hep-lat]].
- [21] P. Boucaud *et al.* [ETM], *Comput. Phys. Commun.* **179** (2008), 695-715 doi:10.1016/j.cpc.2008.06.013 [arXiv:0803.0224 [hep-lat]].
- [22] C. Michael *et al.* [ETM], *PoS LATTICE2007* (2007), 122 doi:10.22323/1.042.0122 [arXiv:0709.4564 [hep-lat]].
- [23] W. Wilcox, [arXiv:hep-lat/9911013 [hep-lat]].
- [24] A. Abdel-Rehim, C. Alexandrou, M. Constantinou, J. Finkenrath, K. Hadjiyiannakou, K. Jansen, C. Kallidonis, G. Koutsou, A. V. Avilés-Casco and J. Volmer, *PoS LATTICE2016* (2016), 155 doi:10.22323/1.256.0155 [arXiv:1611.03802 [hep-lat]].
- [25] C. Alexandrou, M. Constantinou, K. Hadjiyiannakou, K. Jansen and F. Manigrasso, *Phys. Rev. D* **104** (2021) no.5, 054503 doi:10.1103/PhysRevD.104.054503 [arXiv:2106.16065 [hep-lat]].
- [26] M. Constantinou, M. Hadjiantonis, H. Panagopoulos and G. Spanouides, *Phys. Rev. D* **94** (2016) no.11, 114513 doi:10.1103/PhysRevD.94.114513 [arXiv:1610.06744 [hep-lat]].
- [27] M. Gockeler, R. Horsley, H. Oelrich, H. Perlt, D. Petters, P. E. L. Rakow, A. Schafer, G. Schierholz and A. Schiller, *Nucl. Phys. B* **544** (1999), 699-733 doi:10.1016/S0550-3213(99)00036-X [arXiv:hep-lat/9807044 [hep-lat]].

- [28] C. Alexandrou *et al.* [ETM], Phys. Rev. D **95** (2017) no.3, 034505 doi:10.1103/PhysRevD.95.034505 [arXiv:1509.00213 [hep-lat]].
- [29] C. Alexandrou, K. Cichy, M. Constantinou, K. Hadjiyiannakou, K. Jansen, A. Scapellato and F. Steffens, Phys. Rev. D **99** (2019) no.11, 114504 doi:10.1103/PhysRevD.99.114504 [arXiv:1902.00587 [hep-lat]].
- [30] R. D. Ball *et al.* [NNPDF], Eur. Phys. J. C **77**, no.10, 663 (2017) doi:10.1140/epjc/s10052-017-5199-5 [arXiv:1706.00428 [hep-ph]].
- [31] J. J. Ethier, N. Sato and W. Melnitchouk, Phys. Rev. Lett. **119** (2017) no.13, 132001 doi:10.1103/PhysRevLett.119.132001 [arXiv:1705.05889 [hep-ph]].
- [32] H. W. Lin, W. Melnitchouk, A. Prokudin, N. Sato and H. Shows, Phys. Rev. Lett. **120** (2018) no.15, 152502 doi:10.1103/PhysRevLett.120.152502 [arXiv:1710.09858 [hep-ph]].
- [33] A. Buckley, J. Ferrando, S. Lloyd, K. Nordström, B. Page, M. Rüfenacht, M. Schönherr and G. Watt, Eur. Phys. J. C **75** (2015), 132 doi:10.1140/epjc/s10052-015-3318-8 [arXiv:1412.7420 [hep-ph]].
- [34] C. Alexandrou *et al.* [Extended Twisted Mass], Phys. Rev. D **102**, no.9, 094508 (2020) doi:10.1103/PhysRevD.102.094508 [arXiv:2007.13800 [hep-lat]].